Int. J. Electrochem. Sci., 8 **(2013)** 6258 - 6268

International Journal of
ELECTROCHEMICAL
SCIENCE
www.electrochemsci.org

A New Electrolytic Method for On-Site Regeneration of Acidic Copper (II) Chloride Etchant in Printed Circuit Board Production

Zhengyu Yang[1,2], *Chengde Huang*[1], *Xiaoqing Ji*[1,2], *Yuxin Wang*[1,2,*]

[1] School of Chemical Engineering and Technology, Tianjin University, Tianjin 300072, PR China
[2] State Key Laboratory of Chemical Engineering, Tianjin University, Tianjin 300072, PR China
[*]E-mail: yxwang@tju.edu.cn

Received: 24 March 2013 / *Accepted:* 12 April 2013 / *Published:* 1 May 2013

To realize safer, cleaner and yet economically competitive production of printed circuit board (PCB), a simple electrolytic process for simultaneous copper (II) chloride etchant regeneration and copper recovery is proposed and investigated. A three dimensional anode made of carbon felt is used to oxidize copper (I) ions while avoiding oxygen and chloride evolution. To prevent etching of the copper plated on the cathode, the stream fed to the cathode chamber is diluted to 0.5 $mol \cdot L^{-1}$ in copper (II) chloride content, in contrast to 1.7 $mol \cdot L^{-1}$ in the spent etchant. At 300 $A \cdot m^{-2}$ the electrolytic cell has a voltage of 1.63 V and a power consumption of 1.54 $kW \cdot h$ per kilogram of copper recovered. Preliminary studies on cell scale-up and worn carbon felt restoration have also been carried out and the results are promising.

Keywords: PCB, Acidic copper (II) etchant, Regeneration, Waste reduction

1. INTRODUCTION

Spent etchants from printed circuit board (PCB) production are a high concentration hazardous waste. With an annual PCB production approaching to 300 million m^2 in the world [1], around 0.7 million m^3 of the waste would be generated yearly if keeping using the conventional way of maintaining constant etching rate, known as chemical regeneration [2]. The waste generated would be ultimately shipped off-site for reclamation, which usually consumes additional chemicals and results in metal-bearing sludge. Even in situations where the metal and other chemicals are recovered by the waste hauler, this waste stream may be an environmental hazard. Transportation of the spent etchants and their ultimate disposition may pose environmental risks.

To avoid the drawbacks of conventional chemical regeneration, different on-site regeneration methods have been researched and developed [3]. On-site methods usually enable metal recovery and etchant recycling simultaneously and thus substantially reduce the amount of required fresh etchant and other chemicals, while eliminating bulk hazardous waste shipped off-site for reclamation. Besides, an additional revenue from the sale of recovered copper can be gained and the amount of water used and discharged can be reduced [4].

Despite the above mentioned advantages, on-site etchant regeneration has not been widely adopted for technological and/or economical reasons. This is especially true of acidic copper (II) chloride etchant, which accounts for more than 50% of PCB fabrication. Ott et al [5] disclosed an electrolytic method for regenerating spent copper (II) chloride etchant. Copper was formed at a rotating cathode as a powdered slurry, which was then removed by a scraper. Chloride gas evolved from the anode was used to oxidize the copper (I) chloride back to copper (II) chloride. However, the evolution of hazardous chloride could pose great danger. To avoid chloride gas evolution, Oxley et al [6] adopted a flow-through anode where copper (I) ions formed during the etching process are oxidized electrochemically. They further improved the efficiency and quality of cathodic copper plating by including in the regeneration system an additional cell to reduce copper (II) ions into copper (I) ions. But the complexity of the two cell system may further raise the cost of equipment and operation. More recently Zeng et al [7] studied the performance of Ir–Ta oxide-coated anode in oxidizing copper (I) ions from spent acidic copper (II) chloride etchant. The oxidation of copper (I) ions was satisfactory at the currents below 1 $A \cdot dm^{-2}$and cell voltage difference 3.2 V. But the aspect of copper recovery was not touched in their study. Cemeco-FSL [8] has commercialized an etchant regeneration process which features a membrane separated electrolytic cell having one cathode centered between two anodes. While the major benefits of on-site regeneration were realized, also recognized were the inconvenience and problems with the system as exemplified by the requirement of cooling water of below 10°C as well as membrane fouling and puncture.

Besides electrolytic regeneration, other methods developed so far for acidic copper (II) chloride regeneration include solvent extraction [9], cementation [10, 11], copper oxide precipitation [12] and so on [13]. These methods usually suffer from either technical complexity or low economic attractiveness to a greater extent compared with the electrolytic methods. Therefore, it is desirable to find more technically and economically competitive solutions for acidic copper (II) chloride regeneration.

In this study, a new electrolytic method for on-site acidic copper (II) chloride etchant regeneration and copper recovery was proposed and investigated. A process with single electrolytic cell was adopted, with a three dimensional anode constituted by porous carbon felt and an anion exchange membrane to separate the anodic and cathodic chambers of the cell. The effects of stream flow rate and working current density on the performance of etchant regeneration were investigated. In addition, cell scale-up was carried out and electrochemical restoration of worn carbon felt anode was tempted.

2. EXPERIMENTAL

2.1 Electrolysis

The electrolytic cell for acidic copper (II) chloride etchant regeneration was constructed using carbon felt (F-210, Kureha Shanghai, Inc.) as three dimensional anode and copper foil (99wt%, Tianjin AiDaHengSheng Technology Co. Ltd.) as cathode (see Fig.1). The liquid in the anodic and cathodic chambers of the cell was separated by an anion exchange membrane (AMI-7001, Membranes International Inc) to avoid liquid mixing while enabling ionic conduction between the two electrode chambers. The cell has a liquid holdup of around 110 cm^3 and an effective membrane area of 28 cm^2. Imitating the spent copper (II) chloride etchant, Solution A containing 1.7 $mol \cdot L^{-1}$ $CuCl_2$, 0.1$mol \cdot L^{-1}$ CuCl, 2 $mol \cdot L^{-1}$ HCl and 2 $mol \cdot L^{-1}$ NaCl was prepared. The solution was fed to the anode chamber, where copper (I) ions was oxidized to copper (II) ions. Solution B fed to the cathodic chamber is the same as Solution A except that the content of copper (II) chloride is lowered to 0.5 $mol \cdot L^{-1}$ to prevent the etching of copper from cathode [6, 14]. While Solution B were separately prepared in this study, in practical regeneration process it can be obtained during the startup period in which a portion of spent etchant circulates between the cathode chamber and the Solution B container. The detail of the regeneration process was described by Wang[15]. The two streams come out from the anode and cathode chambers were separately collected for easy determination of current efficiencies.

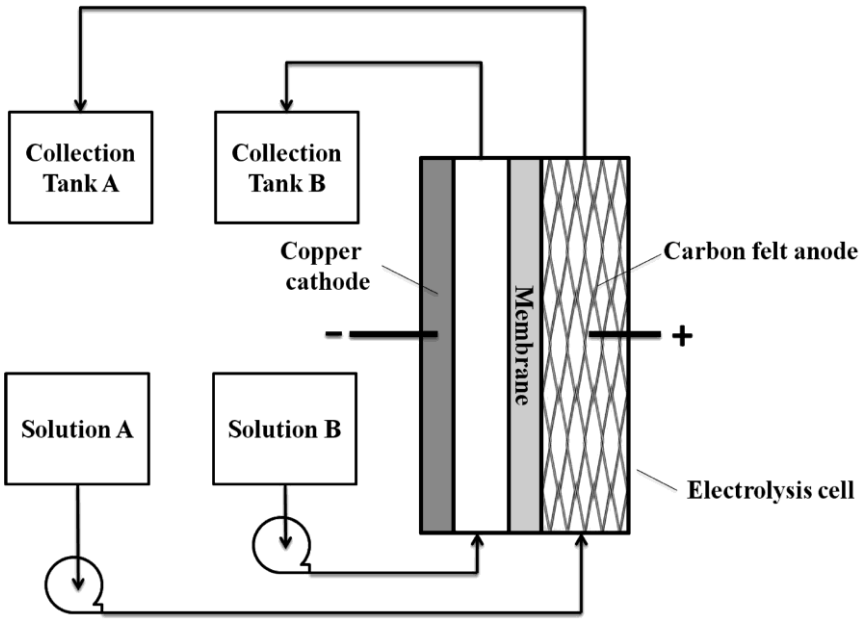

Figure 1. A schematic of the experimental setup for etchant regeneration and copper recovery

Scale-up experiment was carried out using a similar structured cell with an effective membrane area of 300 cm^2 and a liquid holdup of around 1200 cm^3.

The current efficiency at the anode ε_a and cathode ε_c were calculated from the equation

$$\varepsilon_{\mathrm{a}} = \frac{FV_{\mathrm{a}}(C_{\mathrm{a,In,Cu^+}} - C_{\mathrm{a,Out,Cu^+}})}{I} \quad (1)$$

and

$$\varepsilon_{\mathrm{c,Cu}} = \frac{2F\Delta m}{M_{\mathrm{Cu}}It} \quad (2)$$

$$\varepsilon_{\mathrm{c,Cu^+}} = \frac{FV_{\mathrm{c}}(C_{\mathrm{c,Out,Cu^+}} - C_{\mathrm{c,In,Cu^+}})}{I} \quad (3)$$

Where F, I, and V are Faraday constant, current and flow rate at anode or cathode chamber, respectively. C is the copper (II) or copper (I) ion concentration. M_{Cu} is the molecular weight of copper and Δm is the weight amount of copper accumulated at the cathode during the operation time t.

2.2 Determining the concentration of copper (II) and copper (I) ions

The concentration of copper (I) ions in the electrolyte solutions was determined via redox titrimetry [16]. 3 ml of sample, 5 ml of 0.2 mol·L^{-1} $FeCl_3$ solution and one drop of phenanthroline indicator were added to a flask and the mixture was titrated with 0.05 mol·L^{-1} $Ce(SO_4)_2$ standard solution till the color of the mixture turning from red to green. The concentration of copper (I) ions in the sample was calculated from the volume of the standard solution consumed.

To determine the content of copper (II) ions in a electrolyte solution, its copper (I) ion concentration was first measured as above described. Then a calculated amount of $NaClO_3$ was add to the sample solution to oxidize the copper (I) ions into copper (II) ions. The amount of copper (II) ions in the sample was measured via a spectrophotometer (TU-1900, Beijing Purkinje General Instrument Co. Ltd) at 630 nm [17]. Then the original copper (II) ion concentration was determined by subtracting the newly converted from the total.

2.3 Carbon felt anode characterization

Linear sweep voltammetry (Parstat-2273, Princeton Applied Research) was carried out at 0.16 mV·s^{-1} in a flask containing 500 ml of Solution A. A carbon felt sized 1.5 × 1.5 ×1 cm was used as the working electrode. Counter and reference electrodes were chosen to be 3×3 cm platinum foil and Ag/AgCl/3.5mol·L^{-1}KCl, respectively. The apparent surface area of the carbon felt was used to calculate the current density. The morphology of pristine, worn and restored carbon felts was studied using a scanning electronic microscope (S-4800, Hitachi) and the elemental composition at the surface of carbon fibers was detected by a X-ray energy dispersive spectrometer (NORAN System 7, Thermo Scientific).

3. RESULTS AND DISCUSSION

3.1 Linear sweep voltammetry

The linear sweep voltammetry curves of Pt and carbon felt electrodes in the imitated spent copper (II) chloride etchant, Solution A, are shown in Fig. 2 and 3, respectively. It is seen that the oxidation of copper (I) ions begins when the potential at the Pt anode approaches 0.67 V at room temperature (Fig. 2). A limiting current density of 25 $A \cdot m^{-2}$ can be observed at the range of 0.75 V to 1.3 V, which is due to the limited diffusion rate of copper (I) ion toward the anode from bulk solution. Above 1.3 V the current density increases sharply because of oxygen evolution from water. At 50°C a very similar voltammetric curve is obtained (Fig. 2) except that the limiting current density becomes higher, which can be attributed to the increased diffusion rate of copper (I) ions at high temperature. Quite similar temperature dependence of the linear sweep voltammograms were observed in similar and different systems [17, 18].

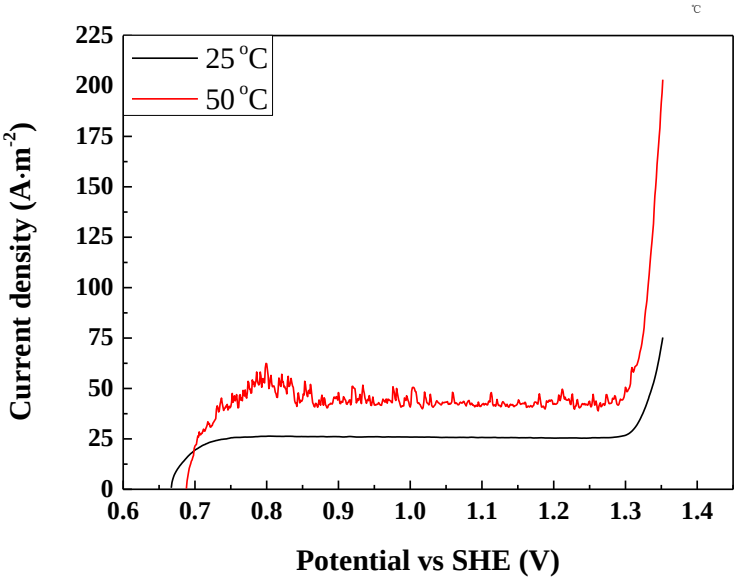

Figure 2. Linear sweep voltammograms of platinum plate in the spent copper (II) chloride etchant Solution A at the scan rate of 0.16 $mV \cdot s^{-1}$ under 25°C and 50°C

Except for similar onset potential of copper (I) ion oxidation, the voltammetric character of carbon felt anode is distinctly different from that of Pt anode (Fig. 2). Much higher apparent current density can be observed with the carbon felt anode (Fig. 3), which possesses considerably larger surface area for electrochemical reaction as compared with the Pt anode. Current due to gas evolution appears at around 1.5 V at room temperature. This suggests that the carbon felt has very high over potential for oxygen and chloride evolution, which is a rather desirable property for the electrode of copper (I) ion oxidation. The limiting current density of copper (I) ion oxidation occurs at around 1.3 V at room temperature, in contrast to 0.75 V in the case Pt anode. No limiting current density and current due to gas evolution can be observed at 50°C even when the potential is over 1.7 V. This indicates that when the condition is more favorable for copper (I) ion oxidation, oxygen and chloride

gas evolution are better constrained. Therefore, the carbon felt anode, with its high surface area and low activity for oxygen and chloride evolution, has the double benefits of promoting copper (I) ion oxidation and curbing hazardous gas generation.

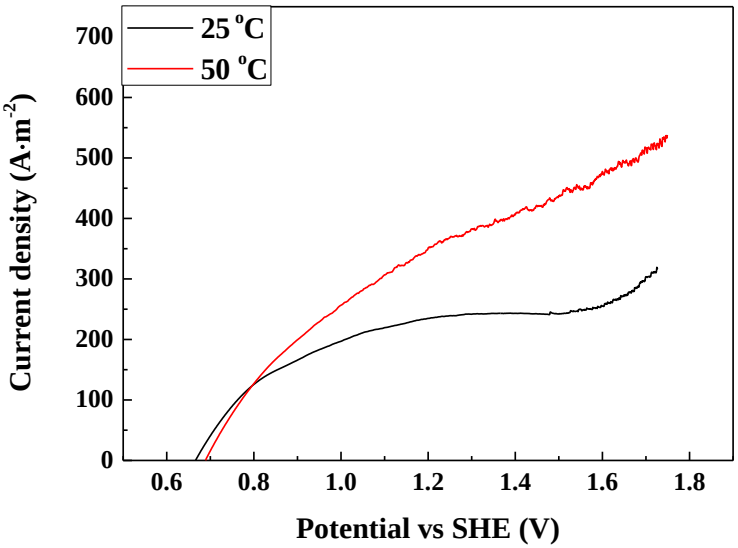

Figure 3. Linear sweep voltammograms of carbon felt anode in the spent copper (II) chloride etchant Solution A at the scan rate of 0.16 $mV \cdot s^{-1}$ under 25°C and 50°C

A similar linear sweep voltammogram was obtained by Oishi, et al. [17], who used carbon felt as an anodic electrode for oxidizing copper (I) ammine complexes. Their carbon felt anode also showed much higher apparent limiting current density over Pt foil anode. However, the limiting current in their system occurred at a much lower potential of around 0.3V, which is related to the open circuit potential of their system. More recently, Zheng, et al. [7] studied the regeneration of acidic copper etching solution with an Ir-Ta oxide-coated anode. Again, similar linear sweep voltammograms were obtained at different temperature. But the limiting current density of their electrode is very low as compared to our carbon felt electrode. Moreover, the Ir-Ta oxide-coated anode showed a low onset potential of gas evolution, which may pose a potential risk in the regeneration process.

3.2 Electrolysis

The performance of our sub-liter scale electrolytic cell in regenerating spent copper (II) chloride etchant and recovering copper is summarized in Table 1. For ensuring copper (II) concentration in cathode chamber to be in optimal range, Flow rates of cathode chamber increased with the increasing of the operation current density [14, 19-21]. The current densities and flow rates of anode chamber were chosen so that anode potential is not well over 1.36 V to ensure no or very low chloride evolution but high enough to effectively oxidize copper (I) ions. The residue concentration of copper (I) ions at the anode chamber is affected by flow rate at a given current density, as evidenced by the experiment 4, 6 and 7. Smaller anodic flow rate leads to lower residue concentration of copper

(I) ions, but higher anodic potential and cell voltage difference, which in turn results in higher specific power consumption of copper recovery and copper (II) chloride etchant regeneration.

It can be noticed from the 6th line of Table1 that the anodic current efficiencies in those experiments are over 100%, which means more copper (I) ions are oxidized to copper (II) ions than calculated from electrons consumption. The extra copper (II) ions are generated because of oxygen ingress [8]:

$$4CuCl + O_2 + 4HCl \rightarrow 4CuCl_2 + 2H_2O \quad (4)$$

We did not tried to prevent oxygen ingress in our experiments as it is hard to avoid in practical etching process. The decrease of anodic current efficiency with current density has to do with the time needed to finish a batch of electrolysis. High flow rates were chosen to accommodate high current density, which usually meant short operation time to empty a tank and thus short time for oxygen ingress. The problem with the chemical oxidation of copper (I) ion is hydrogen chloride drag out and water formation, as indicated in Eq. (4). While the water formed makes up for the water lost by evaporation to some extent, hydrogen chloride needs to be replenished in the practical electrolytic regeneration process. The replenishment does not need in our experiments because they did not involve etchant cycling.

Table 1. A summary of results from subliter-scale electrolytic cell experiments

No.	Current density i /A·m^{-2}	Flow rate of anode chamber v_a /ml·min^{-1}	Flow rate of cathode Chamber v_c /ml·min^{-1}	Anode potential E_a /V	Cell voltage difference ΔE_{cell} /V	Deposited copper mass per unit time m_{Cu} /×10^{-3}kg·h	Current efficiency ε/%			Power consumption of unit copper W_{Cu} /kW·h·kg^{-1}	Concentrations of Cu^+ after electrolysis C_{Cu^+} /mol·L^{-1}
							Anode Cu^+ to Cu^{2+}	Cathode Cu^{2+} to Cu	Cathode Cu^{2+} to Cu^+		
1	100	4.0	0.4	0.897	1.146	0.1114	132.5	31.5	65.1	2.882	0.043
2	200	8.0	0.8	0.998	1.384	0.4287	122.7	62.4	33.5	1.808	0.050
3	250	10.5	1.0	1.026	1.571	0.6119	117.5	73.6	21.7	1.797	0.051
4	300	12.5	1.2	1.096	1.632	0.8880	119.0	88.5	6.7	1.544	0.067
5	400	16.0	1.5	1.375	1.970	1.0141	108.6	73.7	20.3	2.176	0.080
6	300	7.0	1.0	1.230	1.866	0.8261	110.6	83.3	12.2	1.898	0.017
7	300	5.6	1.0	1.437	2.065	0.8366	105.3	82.5	12.6	2.073	0.001

Table 2. A summary of results from liter-scale electrolytic cell experiments

Current density i /A·m^{-2}	Flow rate of anode chamber v_a /ml·min^{-1}	Flow rate of cathode chamber v_c /ml·min^{-1}	Anode potential E_a /V	Cell voltage difference ΔE_{cell} /V	Deposited copper mass per unit time m_{Cu} /×10^{-3}kg·h	Current efficiency ε /%			Power consumption of unit copper W_{Cu} /kW·h·kg^{-1}	Concentrations of Cu^+ after electrolysis C_{Cu^+} /mol·L^{-1}
						Anode Cu^+ to Cu^{2+}	Cathode Cu^+ to Cu^{2+}	Cathode Cu^+ to Cu^{2+}		
250	47.0	10.5	1.011	2.371	7.0544	96.7	77.4	22.4	2.521	0.004
300	56.5	12.0	1.153	2.507	9.9782	97.8	92.8	5.8	2.261	0.003

The performance of liter scale electrolytic cell is shown in Table 2, which indicates that the around ten folds scale-up from the sub-liter cell is satisfactory. The potential at the anode are low enough to avoid gas evolution, while the copper (I) ions in the anolyte are fully oxidized. It is noted, however, that the cell voltage difference and the specific power consumptions of copper recovery are

higher than that in the case of sub-liter cell. This is mainly because of the larger interfacial resistance between the carbon felt and the carbon plate current collector in the liter scale cell. Whereas in the sub-liter cell, the current collector of carbon felt anode is made of Pt wire which results in lower interfacial resistance. Nevertheless, the cell voltage difference is still match lower than 6~10 V as reported in Ref. [8]. This much lower voltage difference would mean higher process safety and lower specific power consumption, thus a competitive advantage of the technology.

3.3 Carbon felt stability and restoration

The performance deterioration of carbon felt electrode after long hours of working under anodic potential was noticed and thus the restoration of worn carbon felt was tried. The carbon felt accumulatively worn for 100 h was restored under a cathodic potential of -3.2 V vs. SHE in 0.1 $mol \cdot L^{-1}$ NaOH electrolyte for 6 h, in order to reduce the oxygen and chloride containing species formed on the felt surface during etchant regeneration. While we have found no previous reports on the electrochemical restoration of carbon felt anode as we did, its underlying principle found applications in the regeneration of various carbon materials, from electrodes to adsorbents [22-24]. Those studies revealed that electrochemical regeneration works by detaching adsorbed species and opening up blocked fine pores, both of which can be expected to happen in carbon felt material.

Overall, the surface morphologies of pristine, worn and restored carbon felt do not have much difference, as shown in Fig. 4 (a), (b) and (c), respectively. But the surface of worn felt fiber (Fig. 4 (b)) is not as smooth as that of pristine fiber (Fig. 4 (a)), and the restoration seems to smoothen the fiber surface to some extent (Fig. 4 (c)). More definite changes are revealed by EDS analysis (Table 3). It shows that the oxygen and chloride contents on the surface of worn carbon felt are noticeably higher than that of pristine carbon felt. Although not fully returned to its original surface composition, the restored carbon felt has obviously lower surface oxygen and chloride contents compared with the worn carbon felt before restoration.

Table 3. A summary of EDS data on the elemental compositions of carbon felt surface

Carbon felt	C/%	O/%	Cl/%
Pristine	~100	<0.5	<0.1
Worn 100 hours	95.7	3.3	0.8
Restored	99.4	<0.5	0.5

The linear sweep voltammetry curves of pristine, worn and restored carbon felt anodes in imitated spent copper (II) chloride etchant at 50°C are compared in Fig. 5. It is seen that a noticeable deterioration of the anode can happen after 100 h of electrolysis. Fortunately, roughly half of the decrease in current density can be regained through the above mentioned simple restoration procedure.

However, the performance deterioration of anode cannot be attributed only to the oxidation of carbon felt. Certain carbon fibers of carbon felt anode can be scoured away from the bulk as electrolyte flowing through it during the electrolysis.

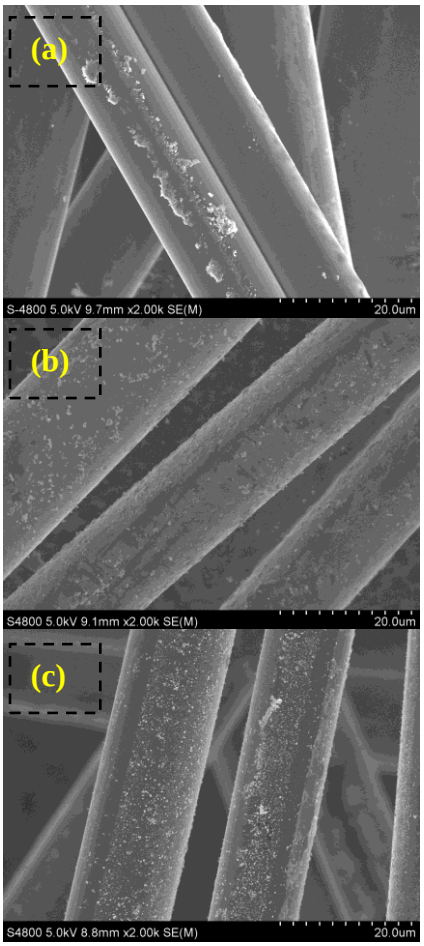

Figure 4. SEM images of (a) pristine, (b) worn 100 h and (c) restored carbon felts

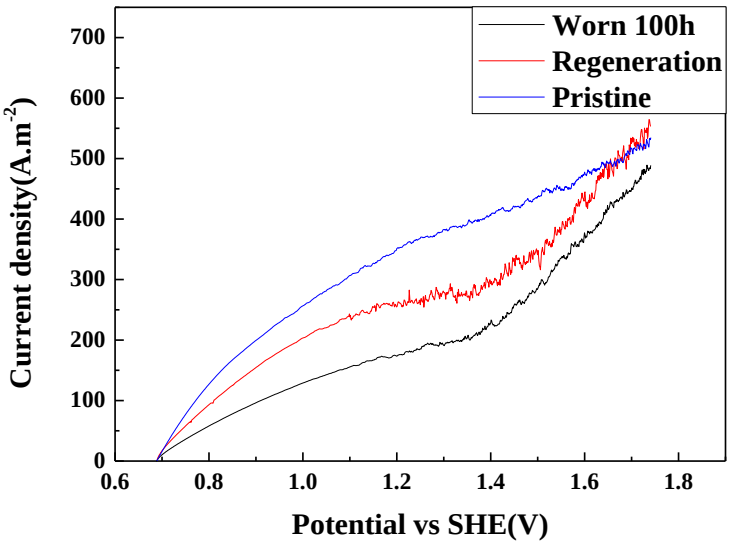

Figure 5. Linear sweep voltammograms of pristine, worn 100 h and restored carbon felt anode in the spent copper (II) chloride etchant Solution A at the scan rate of 0.16 $mV \cdot s^{-1}$ under 50°C

This loss of carbon fibers would cause a decrease of available surface area of the anode, and thus deteriorating its performance. For the same reason, our restoration procedure cannot make the apparent anodic current density returning to its original value, even if the oxygen and chloride containing species formed during etchant regeneration can be fully reduced in the restoration.

4. CONCLUSION

A new electrolytic method for on-site regeneration of acidic copper (II) chloride etchant in PCB production has been proposed and investigated. Carbon felt is chosen as three dimensional anode in order to oxidize copper (I) ions effectively while avoiding gas evolution. Satisfactory etchant regeneration and copper recovery can be simultaneously achieved at considerably lower cell voltage difference and specific power consumption, as compared with the known technology on the market [7, 8]. Furthermore, the price of carbon felt is lower than almost other plate anodes which are used for regeneration spent copper (II) chloride etchant. Preliminary research results on cell scale-up and worn carbon felt restoration are promising.

ACKNOWLEDGEMENT
We acknowledge financial support from the Natural Science Foundation of Tianjin (11JCZDJC23800), Natural Science Foundation of China (2012BGH-0001) and the Program of Introducing Talents of Discipline to Universities (B06006).

Symbols:
C — concentration $mol \cdot L^{-1}$
E — potential & voltage V
F — Faraday's constant $96485 C \cdot mol^{-1}$
I — current A
i — current density $A \cdot m^{-2}$
m — mass kg
M — mole mass $kg \cdot mol^{-1}$
n — electron transfer number
t — time h
V — flow velocity $ml \cdot min^{-1}$
v — scan rate $mV \cdot s^{-1}$
W — energy $kW \cdot h$
ε — current efficiency

References

1. http://www.ipc.org/ContentPage.aspx?pageid=IPC-World-PCB-Production-Report-Shows-19-Percent-Growth-in-2010
2. Q. Yang and N.M. Kocherginsky, *J. Membrane Sci*., 286 (2006) 301.
3. P. Adaikkalam, G. Srinivasan and K. Venkateswaran, *JOM*, 54 (2002) 48
4. O. Cakir, J. Mater. *Process. Technol*., 175 (2006) 63.
5. R. Ott and H. Reith, US Patent 4508599 (1985).

6. J.E. Oxley and R.J. Smialek, US Patent 5705048 (1998).
7. Z. Zheng, Z. Li, H. Yang and G. Zhao, Electroplat. Finish., 29 (2010) 29 (in Chinese).
8. E. Gomes, J. Tandy and J. Siegel, Methuen, Massachusetts, Toxics Use Reduction Institute, University of Massachusetts Lowell (1997).
9. K. Wieszczycka, M. Kaczerewska, M. Krupa and A. Parus, *Sep. Purif. Technol*. 95 (2012) 157.
10. H. Hong, M. Kong, J. Ghu, J. Lee and H. Suk, *J. Mater. Sci. Technol*., 24 (2008) 141.
11. Y. Hung, N. Mohamed and H. Darus, *J. Applied Sci*., 5 (2005) 1328.
12. V.R. Allies, M.F. Lloyd and J.M. Mccarron, US Patent 5560838 (1996).
13. T. Keskitalo, J. Tanskanen and T. Kuokkanen, *Resou. Conserv. and Recy*., 49 (2007) 217.
14. L. Cifuentes, J.M. Casas and J. Simpson, *Chemi. Eng. Sci*., 63 (2008) 1117.
15. Y.X. Wang and Z.Y. Yang, China Patent 201210393174 (2012)
16. State Bureau of Petroleum and Chemical Industries, Cuprous chloride for industrial use, HG/T 2960-2000, 2000 (in Chinese).
17. T. Oishi, M. Yaguchi, K. Koyama, M. Tanaka and J. Lee, *Electrochim. Acta*, 53 (2008) 2585.
18. H. Liu, Q. Xu, C. Yan, Ya. Cao and Y. Qiao, *Int. J. Electrochem. Sci*., 6 (2011) 3483.
19. E. Pellicer1, S. Pane, V. Panagiotopoulou, S. Fusco, K. M. Sivaraman, S. Surinach1, M. D. Baro, B. J. Nelson and J. Sort, *Int. J. Electrochem. Sci.*, (2012) 4014.
20. H.H. A. Rahman, A.H.E. Moustafa, S.M.K. A. Magid, *Int. J. Electrochem. Sci*., 7 (2012) 6959.
21. R. S. Akpanbayev, B. Mishra, A. O. Baikonurova, G. A. Ussoltseva and A. P. Kurbatov, *Int. J. Electrochem. Sci.*, (2013) 3150.
22. A. S. Adekunle, B. B. Mamba, B. O. Agboola and K. I. Ozoemena, *Int. J. Electrochem. Sci.*, 6 (2011) 4388.
23. Y. Chen, X. Zheng and X. Hu, *CIESC J.*, 62 (2011) 102.
24. S.N. Hussaina, H.M.A. Asghara, A.K. Campenb, N.W. Brownb and E.P.L. Roberts, *Electrochim. Acta*, (2013) http://dx.doi.org/10.1016/j.electacta.2013.03.017